RESEARCH ARTICLE | OCTOBER 05 2017

Synthesis and electrochemical characterization of nanosized Li_2MnO_3 cathode material for lithium ion batteries

Shiyou Li; Dan Lei

AIP Conf. Proc. 1890, 040037 (2017)
https://doi.org/10.1063/1.5005239

Synthesis and Electrochemical Characterization of nanosized Li_2MnO_3 Cathode Material for Lithium Ion Batteries

Shiyou Li[a] and Dan Lei[b]

College of Petrochemical Technology, Lanzhou University of Technology, 730050, China

[a] Corresponding author: sylilw@163.com
[b] 709347121@qq.com

Abstract. A simple one-step solid state reaction way of preparing Nano sized Li_2MnO_3 powders is investigated. Synthesized products were characterized by X-ray diffraction (XRD) and scanning electron microscopy (SEM). In addition, we have observed that the inferior electrochemical performance of Li_2MnO_3 upon cycling was attributed to the structural degradation caused by migration of the transition metal (Mn) into the Li layer and repetitive shearing of oxygen layers.

Keywords: Li_2MnO_3; One-step solid state reaction; Lithium-ion batteries.

INTRODUCTION

Lithium manganese oxides $LiMnO_2$, $Li_{0.33}MnO_2$, $LiMn_2O_4$, $Li_2Mn_4O_9$, Li_2MnO_3, etc. are electro active intercalation host materials in lithium cells [1]. Among this family of oxides, Li_2MnO_3 cathode materials attracted much attention for many reasons. First, Li_2MnO_3 itself has a very high theoretical capacity. Thus, many efforts have been done in order to activate and utilize all the Li-ions in Li_2MnO_3 material [2-4]. Second, Li_2MnO_3 is a very interesting electrode material due to its O^{3-} type layered structure and electrochemical behavior with a particular electrochemical mechanism. O_2 releases from the bulk and the intercalation potential decreases, it was generally believed that Mn^{4+} cannot be oxidized to the higher oxidation state as it is electrochemically inactive in Li_2MnO_3[5-7]. It is therefore necessary to investigate Li_2MnO_3 and its properties.

In this study, we have synthesized Nano sized Li_2MnO_3 materials using a relatively simple one-step solid-state reaction method. In addition, we investigated the reasons for the limited capacity observed in experiments and studied the physical parameters and electrochemical performance of Li_2MnO_3 by methods such as X-ray diffractometry (XRD) and scanning electron microscopy (SEM).

EXPERIMENTAL

Synthesis

The Li_2MnO_3 cathode material was synthesized via the one-step solid state reaction. All the reagents used in the experiment were analytical grade. Manganese acetate ($Mn(CH_3COO)_2 \cdot 4H_2O$) and lithium acetate ($CH_3COOLi$) were thoroughly mixed by milling in ethanol for 1 h at a molar ratio of 1:2. The resulting mixture was dried at 75 °C for 12 h, and then annealed at temperatures 700 °C for 10 h in air followed by cooling down to obtain the final Li_2MnO_3 product.

2nd International Conference on Materials Science, Resource and Environmental Engineering (MSREE 2017)
AIP Conf. Proc. 1890, 040037-1–040037-4; https://doi.org/10.1063/1.5005239
Published by AIP Publishing. 978-0-7354-1568-3/$30.00

Cell preparation

Electrochemical tests were performed by the coin cells (2032 type) assembled in an argon glove box. The cathode materials were formed from the active materials, poly (tetrafluoroethylene) binder and acetylene black in 84: 8: 8 by weight ratio. 1 M $LiPF_6$ dissolved in a mixture of ethylene carbonate and diethyl carbonate (1:1, vol. %) was used as the electrolyte between lithium metal anode and cathode material.

Electrochemical measurement

X-ray powder diffraction (XRD) design of sample was analyzed on an X-ray diffract meter (Rigaku, D/Max-2400) with Cu Kα radiation (40 kV). The morphologies of the samples were observed by scanning electron microscopy (SEM, JSM-5600, and Japan). Electrochemical measurements of the cells were carried out on a LAND CT2001A tester (Wuhan, China).

RESULTS AND DISCUSSION

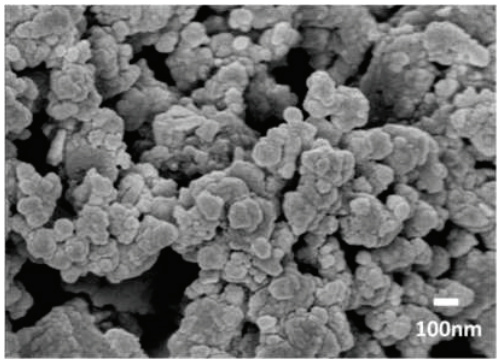

FIGURE 1. Xrd Patterns of Li2mno3 Products.

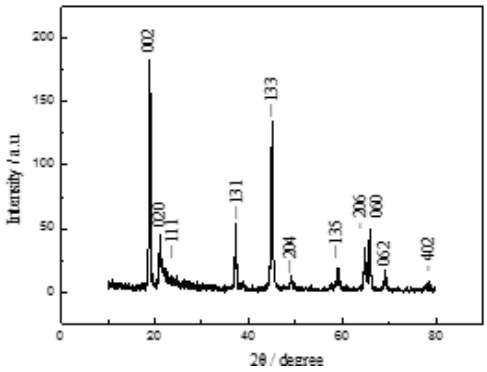

FIGURE 2. Sem Images of Li2mno3 Products.

The XRD diffraction patterns of the prepared Li_2MnO_3 nanoparticles are shown in Fig. 1. The crystal system is modeled as a monoclinic phase (space group: C2/m). All of the diffraction peaks of the prepared samples are well matched with no impurity peaks, indicating that a pure Nano crystalline phase was obtained by the one-step solid state reaction method. The super lattice peaks between 20° and 25° are due to the ordering of Li/M n in the transitional metal layers [8].

Microscopic measurements of the Li_2MnO_3 particles, Fig.2, demonstrate that materials are consisted of small crystallites with a nanometer grain size. From a histogram of the particle-size distribution we concluded that it was represented by nanoparticles with average particle sizes in about 80 nm, such a particle characteristic is beneficial for rapid Li-ion diffusion along the confined dimension.

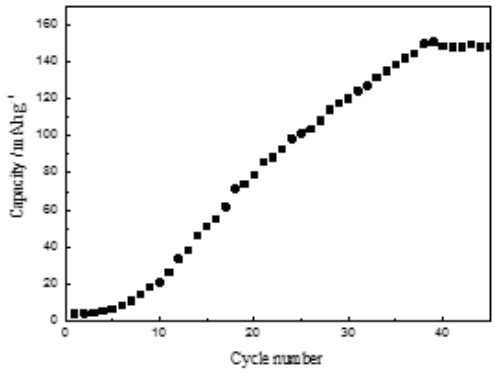

FIGURE 3. Cycling Performance of Li2mno3/Li Cell at 0.2 C.

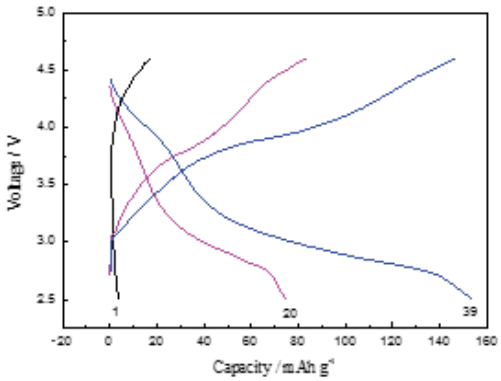

FIGURE 4. Charge and Discharge Curves of Li2mno3/Li Cell at 0.2 C.

Cycling stability measurements of Nano sized Li_2MnO_3 are performed in a potential range of 2.5-4.6 V with a C/5 rate as shown in Fig. 3. It is well-known that the stoichiometric Li_2MnO_3 material commonly shows no electrochemical reaction. Because its charge balance can be expressed as $Li_2^{1+}Mn^{4+}O_3^{2-}$, it is difficult for the lithium ions to insert/extract in the Mn layers between 2.5 V and 4.6 V windows. In this case, the Li/Li_2MnO_3 cell shows an initial charge/discharge capacity (3.8 m Ah g^{-1}) in the first cycle, and then, the capacity is drastically increased up to about 153.7mAh g^{-1} at 39th cycle. The inferior cycling behavior can be ascribed to the dissolution of manganese, the transition from layered to spinel structure and to side reactions related to the decomposition of the electrolyte. The structural transition from a layered to a spinel structure is related to the migration of manganese ions into the lithium layers caused by the release of oxygen [9-11].

Charge-discharge curves with a C/5 rate at 25°C of several Li_2MnO_3 samples are shown in Fig. 4. The initial discharge curves of cell in the 4 V regions could be considered to show the existence and participation of spinel and layered type composite electrodes during cycling. As more lithium ions are inserted into the host structure, the voltage profile undergoes another distinguished voltage plateau around at 3 V. The 3 V plateau is one of the characteristics of the spinel phase, $Li_{1+x}Mn_2O_4$, wherein lithium ions are inserted into the octahedral sites [12]. Notice that the 4 V and 3 V plateau in the charge/discharge curves becomes increasingly flatter with further cycling, which suggests that the structure has slowly transformed into the spinel structure. It confirmed the conclusion that the inferior electrochemical cycling behavior of the Li_2MnO_3 electrode can partly attributed to the formation of a composite structure.

CONCLUSION

In summary, Li_2MnO_3 with 80 nm in particle size can be obtained via one-step solid state reaction. The resulting material exhibits a very low initial charge/discharge capacity in the first cycle, but the capacity is drastically increased up to about 153.7 mAh g^{-1} at 39th cycle. The inferior electrochemical performance of Li_2MnO_3 upon cycling is attributed to the structural degradation caused by migration of the transition metal (Mn) into the Li layer and repetitive shearing of oxygen layers.

ACKNOWLEDGMENTS

This work was supported by the Natural Science Foundation of China (No. 21406100 and 51502124), the Supporting Plan for Youth Innovative Talents of Long Yuan, and the Foundation for Innovation Groups of Basic Research in Gansu Province (No. 1606RJIA322).

REFERENCES

1. Amalraj SF, Sharon D, Talianker M, Julien CM, Burlaka L, Lavi R, et al. Electrochemical Acta **97**, 259-270 (2013).
2. Lim JM, Kim D, Lim YG, Park MS, Kim YJ, Cho M, et al. Chemelectrochem **3**, (2016).
3. Zhao W, Xiong L, Xu Y, Xiao X, Wang J, Ren Z. Journal of Power Sources **330**, 37-44 (2016).
4. Zhang X, Luo D, Li G, Zheng J, Yu C, Guan X, et al. Journal of Materials Chemistry A **1**, 9721(2013).
5. Wu X, Li H, Fei H, Zheng C, Wei M. New J Chem **38**, 584-587 (2014).
6. Cheng M, Tang W, Sun Y, Zhu K. RSC Adv **5**, 71088-71094 (2015).
7. Shimoda K, Oishi M, Matsunaga T, Murakami M, YAMANAKA K, Arai H, et al. Journal of Materials Chemistry A, (2017).
8. Wang F, Xiao S, Li M, Wang X, Zhu Y, Wu Y, et al. Journal of Power Sources **287**, 416-421 (2015).
9. Klein A, Axmann P, Yada C, Wohlfahrt- Mehrens M. Journal of Power Sources **288**, 302-307 (2015).
10. Yabuuchi N, Kubota K, Aoki Y, Komaba S. Journal of Physical Chemistry C **120**, (2016).
11. Gao Y, Ma J, Wang Z, Lu G, Chen L. Physical Chemistry Chemical Physics Pccp **19**, 7025 (2017).
12. Park SH, Sato Y, Kim J, Lee YS. Materials Chemistry & Physics **102**, 225-230 (2007).